

Polymer Winding Numbers and Quantum Mechanics*

David R. Nelson⁽¹⁾,

and Ady Stern⁽²⁾

⁽¹⁾*Lyman Laboratory of Physics, Harvard University, Cambridge, MA 02138*

⁽²⁾*Department of Condensed Matter Physics, Weizmann Institute of Sciences, Rehovot 76100,*

Israel

(October 6, 2018)

Abstract

The winding of a single polymer in thermal equilibrium around a repulsive cylindrical obstacle is perhaps the simplest example of statistical mechanics in a multiply connected geometry. As shown by S.F. Edwards, this problem is closely related to the quantum mechanics of a charged particle interacting with a Aharonov-Bohm flux. In another development, Pollock and Ceperley have shown that boson world lines in $2 + 1$ dimensions with periodic boundary conditions, regarded as ring polymers on a torus, have a mean square winding number given by $\langle W^2 \rangle = 2n_s \hbar^2 / mk_B T$, where m is the boson mass and n_s is the superfluid number density. Here, we review the mapping of the statistical mechanics of polymers with constraints onto quantum mechanics, and show that there is an interesting generalization of the Pollock-Ceperley result to directed polymer melts interacting with a repulsive rod of radius a . When translated into boson language, the mean square winding number around the rod for a system of size R perpendicular to the rod reads $\langle W^2 \rangle = \frac{n_s \hbar^2}{2\pi m k_B T} \ln(R/a)$. This result is directly applicable to vortices in Type II superconductors in the presence of columnar defects. An external current passing through the rod couples directly to the winding number in this case.

I. INTRODUCTION

The study of the statistical mechanics of polymers in multiply connected geometries began many years ago with work by S.F. Edwards and by S. Prager and H.L. Frisch [1,2]. The simplest nontrivial geometry consists of a polymer interacting with a repulsive rod, and the corresponding path integrals can be analyzed via an elegant analogy with the physics of a quantum mechanical particle interacting with a solenoidal vector potential [3]. The mean square winding number of the polymer around the rod, and other interesting quantities can be computed for this problem [4]. The physics bears a close mathematical relation to the famous Aharonov-Bohm effect for a real quantum mechanical particle interacting via its charge with a tube of magnetic flux [5].

More recently, Pollock and Ceperley have studied the winding numbers with respect to periodic boundary conditions for boson world lines in the Feynman path integral formulation of superfluidity in two dimensions [6]. The physics here is equivalent to *many* ring polymers interacting on the surface of a torus. The mean square winding number of the world lines around the torus can be expressed exactly in terms of the renormalized superfluid density of the equivalent boson system [7].

Winding numbers and the statistical mechanics of many polymer-like objects are also relevant to the physics of vortex lines in Type II superconductors [8]. Here, thermal fluctuations in the trajectory of a vortex defect in the superconducting order parameter can be described by a Feynman path integral for an elastic string. A collection of many such lines behaves like a directed polymer melt, with the added complication of a quenched random disorder potential [9]. Point-like disorder is always present to some degree due, for example, to quenched fluctuations in the concentration of oxygen vacancies in the high temperature cuprate superconductors. Drossel and Kardar have studied how the winding number distribution of a single directed polymer around various obstacles is affected by point-like disorder [10].

Dramatic improvements in the pinning efficiency of vortex lines have recently been

achieved via the introduction of *columnar* damage tracks created by heavy ion irradiation. If the concentration of damage tracks (assumed to pass completely through the sample) exceeds the number flux lines, there is a low-temperature “Bose glass” phase, in which every vortex is trapped on a columnar defect [11]. At high temperatures, the vortices delocalize in an entangled flux liquid. If these vortex trajectories are viewed as the world lines of quantum mechanical particles, the physics in thick samples becomes equivalent to that of a low temperature boson superfluid in $2 + 1$ dimensions [9].

In this paper, we discuss how to compute polymer winding numbers from the Hamiltonian formulation of quantum mechanics, keeping in mind applications to vortex lines interacting with many columnar defects. A random distribution of columns maps onto a time-independent random potential in the quantum mechanical analogy [11]. We assume high temperatures, and samples which are clean before irradiation, so that point disorder is negligible and the usual Abrikosov flux lattice is either melted by thermal fluctuations or destroyed by the columnar disorder. An experimental realization of a multiply connected geometry for thermally excited flux lines is illustrated in Fig. 1. Superimposed on a dilute concentration of parallel columnar defects scattered randomly throughout a superconducting sample is a slender tube in which the columns are very dense. Such a “tube of columns” could be made by covering a sample with a mask containing a small submicron hole during irradiation with a strong dose of heavy ions. Imagine that this sample is first subjected to a very large magnetic field, such that the density of flux lines is approximately equal to the density of columns in the tube. It should be possible to choose the temperature such that the vortices in the tube are in the Bose glass phase, while those outside constitute a flux liquid. The many trapped vortices inside the tube should then present a virtually impenetrable barrier to the thermally excited vortex lines outside. The concentration of lines in the liquid outside this repulsive cylindrical obstacle could be varied by decreasing the magnetic field. Because flux creep in the Bose glass phase is quite slow [8,11], the concentration of vortices in the tube should remain approximately constant as a field is turned down, leaving the barrier almost unchanged.

We shall explore the winding number fluctuations of the vortices with respect to the repulsive cylindrical tube in this experiment. As discussed below, a current passing through the tube couples directly to the net vortex winding number, and the mean square winding number of the unperturbed system gives the linear response of the net winding number to this current. (See Fig. 2) Such a current acts like an imaginary vector potential when this problem is mapped onto quantum mechanics [11]. Winding of vortices around a thin repulsive obstacle (or a set of such obstacles) could be probed via double-sided flux decorations [12] or indirectly by monitoring the flux flow resistivity in the plane perpendicular to the common direction of the applied field and the columns. The extra entanglements induced by the longitudinal current should impede vortex transport in this plane, and it would be especially interesting to look for changes in the in-plane resistivity as a function of the current through the tube [13]. This resistance should drop with increasing longitudinal current through the tubes, due to the enhanced vortex winding about the obstacle.

In section II, we briefly review the Feynman path integral description of bosons in $2 + 1$ dimensions, and discuss the Pollack-Ceperley result for the winding numbers of bosons on a torus. We then describe the closely related statistical mechanics of directed polymer melts and vortex lines, and show how a current through a cylindrical obstacle couples to the winding number. In section III, we treat winding number statistics for isolated polymers both with and without columnar pin disorder. Results for *many* polymers or flux lines winding about an obstacle are presented in section IV.

II. TWO-DIMENSIONAL BOSONS AND DIRECTED POLYMER MELTS

A. Boson Statistical Mechanics

The partition function for a set of N nonrelativistic bosons interacting with pair potential $V(r)$ reads

$$\mathcal{Z} = \text{Tr}' \{ e^{-\beta \hat{\mathcal{H}}_b} \}, \quad (2.1)$$

where $\beta = 1/k_B T$ and the boson Hamiltonian operator is

$$\hat{\mathcal{H}}_b = \sum_{j=1}^N \frac{-\hbar^2}{2m} \nabla_j^2 + \frac{1}{2} \sum_{i \neq j} V(|\mathbf{r}_i - \mathbf{r}_j|). \quad (2.2)$$

The prime on the trace means that only symmetrized boson eigenfunctions are to be included in the partition sum, and we shall focus on particles in two space dimensions. This trace can be rewritten in terms of a Feynman path integral by breaking up $\exp[-\beta \hat{\mathcal{H}}]$ into M pieces ($M \gg 1$),

$$e^{-\beta \hat{\mathcal{H}}_b} = e^{-\Delta\tau \hat{\mathcal{H}}_b} e^{-\Delta\tau \hat{\mathcal{H}}_b} \dots e^{-\Delta\tau \hat{\mathcal{H}}_b} \quad (M \text{ times}) \quad (2.3)$$

where $\Delta\tau M = \beta$. Upon inserting complete sets of position states between various terms in the product and taking the limit $M \rightarrow \infty$, the boson partition function \mathcal{Z}_b may be expressed as an integral over a set of polymer-like trajectories $\{\mathbf{r}_j(\tau) = [x_j(\tau), y_j(\tau)]\}$ in imaginary time [14],

$$\begin{aligned} \mathcal{Z}_b = \frac{1}{N!} \sum_P \prod_{j=1}^N \mathcal{D}\mathbf{r}_j(\tau) \exp \left[-\frac{1}{2} \frac{m}{\hbar} \sum_{j=1}^N \int_0^{\beta\hbar} \left(\frac{d\mathbf{r}_j}{d\tau} \right)^2 d\tau \right. \\ \left. - \frac{1}{\hbar} \sum_{i>j} \int_0^{\beta\hbar} V(|\mathbf{r}_i(z) - \mathbf{r}_j(z)|) d\tau \right] \end{aligned} \quad (2.4)$$

The normalized sum over permutations P insures that only boson eigenfunctions contribute to the sum, where the trajectories obey a type of periodic boundary condition,

$$\{\mathbf{r}_j(\beta\hbar) = P[\{\mathbf{r}_i(0)\}], \quad (2.5)$$

and the operator P permutes the set of starting points $\{\mathbf{r}_i(0)\}$.

An approximate picture of the polymer statistical mechanics problem represented by (2.4) can be constructed as follows [14]: Provided interaction effects are not too large, each ‘‘polymer’’ simply diffuses in the imaginary time variable τ ,

$$\langle |\mathbf{r}_j(\tau) - \mathbf{r}_j(0)|^2 \rangle \approx 2 \frac{\hbar}{m} \tau \quad (2.6)$$

where \hbar/m plays the role of a diffusion constant. When the temperature is high, only the identity permutation contributes to Eq. (2.4). When projected onto the (x, y) -plane, the

boson trajectories then behave like small *ring* polymers of typical transverse size given by the thermal deBroglie wavelength Λ_T ,

$$\begin{aligned}\Lambda_T^2 &\equiv 2\pi\hbar^2/mk_B T \\ &\sim \langle |\mathbf{r}_j(\tau) - \mathbf{r}_j(0)|^2 \rangle_{\tau=\beta\hbar}.\end{aligned}\tag{2.7}$$

At temperatures low enough so that $\Lambda_T \gtrsim n^{-1/2}$, where n is the particle number density, complicated cyclic permutations appear, as the trajectories coalesce to form much larger rings. Feynman suggested in 1953 that the lambda transition from a normal bulk liquid of He^4 to a superfluid is associated with a dramatic proliferation in the number and length of such cooperative ring exchanges [15].

Now, following Pollock and Ceperley, consider what happens when the excursions of the bosons in the xy -plane occur in a two-dimensional periodic box of size D [6,7] (see Fig. 3). The permutation requirement (2.6) describing periodic boundary conditions in the τ -direction remains in effect. At high temperatures, virtually all ring polymers return to their initial positions $\{\mathbf{r}_i(0)\}$ when $\tau = \beta\hbar$, and the spatial periodic boundary conditions are unimportant. In the low temperature limit, however, ring exchanges lead to huge composite trajectories which typically wrap completely around the torus embodied in the (x, y) -plane periodic boundary conditions. The collection of cyclic boson trajectories can be classified by a dimensionless topological invariant, the vector winding number \mathbf{W} ,

$$\mathbf{W} = \frac{1}{\sqrt{\Omega}} \sum_{j=1}^N [\mathbf{r}_j(\beta\hbar) - \mathbf{r}_j(0)]\tag{2.8}$$

where $\Omega = D^2$ is the cross-sectional area of a square box with periodic spatial boundary conditions. In evaluating Eq. (2.8), we imagine that the $\{\mathbf{r}_j(\tau)\}$ pass smoothly into neighboring periodic cells, without invoking the periodic boundary conditions (see Fig. 3). Consider the mean square winding number $\langle \mathbf{W}^2 \rangle$, where the angular brackets represent a path integral weighted by the exponential factor in Eq. (2.4) and divided by the boson partition function. Ring polymers which do not wrap completely around the torus make no contribution to Eq. (2.8). However, at temperatures low enough so that $\Lambda_T \gg n^{-1/2}$, virtually all

trajectories belong to a cycle with a nontrivial winding number. We can then regard Eq. (2.8) as a normalized N -step random walk with typical step size Λ_T , and estimate that $\langle \mathbf{W}^2 \rangle \approx \frac{N\Lambda_T^2}{\Omega} = 2\pi n\hbar^2/mk_B T$, where $n = N/\Omega$ is the number density of bosons. Pollock and Ceperley showed that $\langle \mathbf{W}^2 \rangle$ is in fact *exactly* related to the *superfluid density* n_s of the equivalent boson system,

$$\begin{aligned} \langle \mathbf{W}^2 \rangle &= 2n_s(T)\hbar^2/mk_B T \\ &= 2n_s(T)(\hbar^2/m)\beta. \end{aligned} \tag{2.9}$$

The implications of this remarkable connection between a *topological invariant* for a set of ring polymers on a torus and the *superfluid density* of the equivalent set of bosons is summarized in Fig. 4, where $\langle \mathbf{W}^2 \rangle$ is shown as a function of β , which is proportional to the number of “monomers” if the trajectories are viewed as ring polymers. Translational invariance of the boson system in the absence of disorder implies that $\lim_{T \rightarrow 0} n_s(T) = n$, [16], so we know that $\langle \mathbf{W}^2 \rangle$ diverges linearly with β as $\beta \rightarrow \infty$, with slope given exactly by $2n\hbar^2/m$. The existence of a sharp Kosterlitz-Thouless phase transition in superfluid helium films, moreover, implies that there must be a singularity in $\langle \mathbf{W}^2 \rangle$: This quantity *vanishes* below a critical value β_c , and the universal jump discontinuity in the superfluid density [17], $\lim_{T \rightarrow T_c^-} n_s(T)/T = \frac{2}{\pi} k_B \frac{m}{\hbar^2}$, implies the exact result [6]

$$\lim_{\beta \rightarrow \beta_c^+} \langle \mathbf{W}^2 \rangle = \frac{4}{\pi}. \tag{2.10}$$

Feynman hoped that his “cyclic ring exchange” picture of superfluidity could be used to understand the lambda transition in He^4 which was a quite mysterious phenomenon in 1953 [14,15]. Here, the sophisticated understanding of vortex unbinding transitions in He^4 films developed in the past 25 years (using other methods) has been used to make a prediction about a topological quantity, the winding number.

Equation (2.9) allows winding number statistics extracted from computer simulations of bosons with periodic boundary conditions to be converted into measurements of the superfluid density [7]. It can be used, in particular, to probe the reduction in the superfluid

density of helium films due to substrate disorder near $T = 0$. A disordered substrate potential maps onto randomness *correlated* along the imaginary time direction τ in the 2+1-dimensional world line picture of boson physics. The winding number fluctuations are reduced because this correlated randomness reduces the wandering of the boson world lines.

B. Directed Polymer Melts

One might think that the results described above would be applicable, at least in principle, to real ring polymers on the surface of a torus, whose fluctuations include fusing together to form large rings, similar to sulfur ring polymers in equilibrium [18]. Unfortunately, the boson model as applied to ring polymers is unrealistic: The individual “monomers” within a ring, indexed by the imaginary time coordinate τ in Eq. (2.4), are noninteracting, so there is no intra-chain self-avoidance. The only *inter*polymer interactions, moreover, occur between monomers with *same* imaginary time coordinate, which is also unrealistic for a melt of ring polymers.

The physics of directed polymer melts, on the other hand, is much closer to that of real bosons. Because the polymers are directed, interpolymer interactions at the same “imaginary time” coordinate dominate the physics. Vortex lines in superconductors provide an excellent physical realization of this system, but examples can also be found in polymer nematics in strong external magnetic or electric fields [19]. Consider a collection of N vortex lines or polymers in three space dimensions, labelled by x , y and τ (see Fig. 5). We assume that these lines are stretched out on average along the τ axis, so that they can be described by single-valued trajectories $\{\mathbf{r}_j(\tau)\}$. The partition function is a multidimensional path integral, similar to Eq. (2.4),

$$\mathcal{Z} = \prod_{j=1}^N \int \mathcal{D}\mathbf{r}_j(\tau) \exp[-F/T] \quad (2.11a)$$

where

$$F = \frac{1}{2}g \sum_{j=1}^N \int_0^L \left(\frac{d\mathbf{r}_j}{dz} \right)^2 d\tau + \sum_{j=1}^N \int_0^L U(\mathbf{r}_j) d\tau + \sum_{i>j} \int_0^L V(|\mathbf{r}_i - \mathbf{r}_j|) d\tau. \quad (2.11b)$$

Here, the mass m in the boson problem has been replaced by a line tension g , \hbar has been replaced by the temperature T and the polymer system thickness L plays the role of $\beta\hbar$ for the bosons. Unless indicated otherwise, we shall henceforth use units such that $k_B = 1$. $V(r)$ is a repulsive interparticle potential and $U(\mathbf{r})$ represents the random potential due to columnar pins (not shown in Fig. 5). Both $V(r)$ and $U(\mathbf{r})$ are independent of τ . This approximation is quite reasonable for directed polymer melts and vortex lines in $2 + 1$ dimensions, provided $\langle |\frac{d\mathbf{r}}{dz}|^2 \rangle$, the mean square tilt away from the z axis, is small [11].

The statistical mechanics of directed polymers differs from that for bosons due to the absence of periodic boundary conditions in the “imaginary time” direction τ : we assume free boundary conditions in Eq. (2.11a), i.e., we integrate freely over the starting and end points of the polymers. Hence there is no sum over permutations and no condition analogous to Eq. (2.5). This change, however, is less severe than one might think. Indeed, the directed polymer partition function can be written in a form similar to Eq. (2.1), [9]

$$\mathcal{Z} = \prod_{j=1}^N \int d\mathbf{r}'_j \prod_{j=1}^N \int d\mathbf{r}_j \langle \mathbf{r}'_1 \cdots \mathbf{r}'_N | e^{-\hat{\mathcal{H}}L/T} | \mathbf{r}_1 \cdots \mathbf{r}_N \rangle \quad (2.12)$$

where

$$\hat{\mathcal{H}} = -\frac{T^2}{2g} \sum_{j=1}^N \nabla_j^2 + \sum_{j=1}^N U(\mathbf{r}_j) + \sum_{i>j} V(|\mathbf{r}_i - \mathbf{r}_j|), \quad (2.13)$$

and the states $|\mathbf{r}_1 \cdots \mathbf{r}_N\rangle$ and $\langle \mathbf{r}'_1 \cdots \mathbf{r}'_N|$ describe entry and exit points for the polymers or vortices at the top and bottom of the system. The Hamiltonian \mathcal{H} is identical to the Hamiltonian \mathcal{H}_b in Eq. (2.2), provided we introduce a disorder potential $U(\mathbf{r})$ to model the effect of, say, a random substrate on the bosons. Because the initial and final states involve *symmetric* integrations over the entry and exit points, only boson eigenfunctions contribute to the statistical mechanics defined by Eq. (2.12). As, $L \rightarrow \infty$, the physics will be dominated by a bosonic ground state and bosonic low-lying excitations, just as in Eq. (2.1). Thus, the precise choice of boundary condition is irrelevant in the “thermodynamic limit” of large system sizes.

Can one define meaningful “winding number” problems for directed polymers with free ends? Because we are no longer dealing with ring polymers, the “winding number” \mathbf{W} in

Eq. (2.8) (with $\beta\hbar$ replaced by L) no longer has a precise topological meaning, even for periodic boundary conditions in the space-like directions. One can, however, still define and estimate the order of magnitude of the fluctuations in \mathbf{W} as before. In terms of quantities appropriate for directed polymer melts, we have, up to constants of order unity

$$\langle \mathbf{W}^2 \rangle \approx nTL/g, \quad (2.14)$$

where n is the areal number density of polymers in a constant τ cross section. As illustrated (in the absence of a disorder potential) in Fig. 4, we expect that this quantity is nonzero for *all* values of $L \equiv \beta\hbar > 0$. Although the curves for directed polymers and bosons should agree when L and $\beta\hbar$ are large, there is no reason to expect a sharp Kosterlitz-Thouless phase transition for “bosons” with open boundary conditions [20]. The winding number variance for real bosons only vanishes identically for $\beta < \beta_c$ because the contribution to \mathbf{W} from “ring polymer” trajectories which are not wrapped completely around the torus is exactly zero. There is no such condition for the open boundary conditions appropriate to a directed polymer melt.

C. Winding Around an Obstacle

A more interesting case is the winding number distribution for many directed polymers in a disorder potential and interacting with a repulsive cylindrical obstacle. As discussed in the Introduction, this problem has a direct physical realization in the context of thermally excited vortex lines. The combination of a disorder potential and repulsive barrier is illustrated in Fig. 1. We model a repulsive obstacle by modifying the disorder potential in Eqs. (2.11b) and (2.13),

$$U(\mathbf{r}) \rightarrow U(\mathbf{r}) + U_B[\mathbf{r}(\tau)], \quad (2.15)$$

where the barrier potential $U_B(\mathbf{r})$ (centered on the origin) is, e.g.,

$$U_B(r) = \begin{cases} \infty, & r < a \\ 0, & \text{otherwise.} \end{cases} \quad (2.16)$$

This problem is a natural generalization to many directed lines of the original multiply connected geometry problem for single polymers of Edwards [1] and of Prager and Frisch [2]. The (scalar) winding number with respect to the obstacle at the origin is now

$$\mathbf{W} = \sum_{j=1}^N \int_0^L d\tau \mathbf{A}[\mathbf{r}_j(\tau)] \cdot \frac{d\mathbf{r}_j}{d\tau}, \quad (2.17)$$

where the “vector potential” $\mathbf{A}(r)$ is [1]

$$\mathbf{A}(\mathbf{r}) = \frac{\hat{\boldsymbol{\tau}} \times \mathbf{r}}{2\pi r^2}. \quad (2.18)$$

The boundary conditions along the τ direction can be periodic or open [3]. Periodic boundary conditions would imply integer winding numbers, but the noninteger winding numbers which characterize open boundary conditions are of direct physical interest for vortices, as we now explain.

A current in the τ direction through a cylindrical obstacle couples directly to the winding number of vortices outside in Type II superconductors. To see this, assume that the current is entirely confined to the cylinder, i.e., it cannot penetrate into the remainder of the sample. This “confined current approximation” should be applicable to a tube of columnar pins filled with pinned vortices in the bose glass phase, provided its conductivity is much higher than that of the flux liquid outside. Essentially infinite conductivity can be arranged in the tube because irradiation to produce columnar defects with matching field ~ 4 Tesla typically shifts the irreversibility temperature by 5–20°K. Choosing a temperature *above* the irreversibility line of the lightly irradiated region outside the tube but *below* the Bose glass transition inside insures that essentially all the current is confined to the tube. Under these conditions the additional free energy F of the vortices due the current is given by [21]

$$\delta F = -\frac{1}{4\pi} \int' d^2r \int_0^L d\tau \mathbf{H}_{\text{ext}}(\mathbf{r}) \cdot \mathbf{B}_{\perp}(\mathbf{r}, \tau) \quad (2.19)$$

where $\mathbf{H}_{\text{ext}}(\mathbf{r})$ is the field due to the extra current I through the wire

$$\mathbf{H}_{\text{ext}}(\mathbf{r}) = \frac{2I}{c} \frac{\hat{\boldsymbol{\tau}} \times \mathbf{r}}{r^2}, \quad (2.20)$$

and the prime on the integration means that the region inside the obstacle is excluded. The perpendicular component of the magnetic field \mathbf{B}_\perp due to the vortices obeys the anisotropic London equation [22]

$$\mathbf{B}_\perp(\mathbf{r}, \tau) = \phi_0 \sum_{j=1}^N \frac{d\mathbf{r}_j}{d\tau} \delta^{(2)}[\mathbf{r} - \mathbf{r}_j(\tau)] + \frac{M_\tau}{M_\perp} \lambda^2 \nabla_\perp^2 \mathbf{B}_\perp(\mathbf{r}, \tau) + \lambda^2 \partial_\tau^2 \mathbf{B}_\perp(\mathbf{r}, \tau), \quad (2.21)$$

where ϕ_0 is the flux quantum, $\frac{M_\tau}{M_\perp}$ is the mass anisotropy and λ is the screening length in the direction perpendicular to $\hat{\tau}$. Upon substituting Eqs. (2.20) and (2.21) into (2.19), integrating by parts and noting that $(\frac{M_\tau}{M_\perp} \lambda^2 \nabla_\perp^2 + \lambda^2 \partial_\tau^2) \mathbf{H}_{\text{ext}}(\mathbf{r}) = 0$ in the domain of integration, we find that

$$\begin{aligned} \delta F &= -\frac{I\phi_0}{c} \sum_{j=1}^N \int_0^L d\tau \frac{\hat{\tau} \times \mathbf{r}_j}{2\pi r_j^2} \cdot \frac{d\mathbf{r}_j}{d\tau} \\ &\equiv -\gamma W, \end{aligned} \quad (2.22)$$

where we have defined a winding number coupling constant γ ,

$$\gamma = I\phi_0/c. \quad (2.23)$$

Consider now the mean winding number $\langle W \rangle$ induced by the current for vortices outside the obstacle. Upon incorporating an additional factor $e^{-\delta F/T}$ into the Boltzmann weight in (2.11a), we have, upon expanding $\langle W \rangle$ to leading order in the current,

$$\langle W \rangle = \frac{\phi_0}{2\pi cT} \langle W^2 \rangle|_{I=0} I. \quad (2.24)$$

Thus the equilibrium winding number *fluctuations* $\langle W^2 \rangle|_{I=0}$ determine the linear response of the net winding number to an external current.

III. WINDING NUMBER AND QUANTUM MECHANICS: SINGLE POLYMER IN A CYLINDRICAL SHELL

We now study the winding number fluctuations of a single directed polymer, moving on average along the τ axis, and interacting with a repulsive cylindrical obstacle of radius a

centered on the origin of an (x, y) plane perpendicular to $\hat{\tau}$. As discussed above, many of the results are directly applicable to vortex filaments in superconductors. We use the original method of Edwards [1], which maps the generating function for winding numbers onto the quantum mechanics of particles interacting with a solenoidal vector potential. Although winding of a single polymer is simple and relatively well understood [1–4,10], we review the basic results to illustrate the method and discuss effects due to columnar pins outside the obstacle. We use the *directed* polymer notation discussed at the end of section II because the neglect of self-avoidance is justified in this case. The single line results would, however, apply in principle to a “phantom” polymer without self-avoidance in two dimensions interacting with a repulsive disk and a random substrate potential. We defer new results for *many* directed polymers to section IV. We shall, for simplicity, usually impose periodic boundary conditions in the τ direction. This choice should not affect the results for $\langle W^2 \rangle$ in the limit of large sample thicknesses L . For a systematic study of the effects of different boundary conditions in the context of the boson mapping, see ref. [23].

A. Winding Number Formalism

Consider the winding number (2.17), specialized to the case of a single directed polymer with trajectory $\mathbf{r}(\tau)$,

$$W = \int_0^L d\tau \mathbf{A}[\mathbf{r}(\tau)] \cdot \dot{\mathbf{r}}(\tau) \quad (3.1)$$

with $\mathbf{A}(\mathbf{r}) = \frac{\hat{\tau} \times \mathbf{r}}{2\pi r^2}$ and $\dot{\mathbf{r}}(\tau) = d\mathbf{r}/d\tau$. Note that $\mathbf{A}(\mathbf{r})$ is the electro-magnetic vector potential that would have been present had we replaced the cylindrical obstacle by a solenoid enclosing one unit of magnetic flux. If we then regard τ as time, our expression for W becomes the quantum mechanical Aharonov-Bohm phase accumulated by a particle of unit charge traversing a path $\mathbf{r}(\tau)$, due to its interaction with the solenoid. As noted by Aharonov and Bohm [5], this phase is indeed the winding number, which is an integer for periodic boundary conditions, but can assume arbitrary values otherwise.

Our interest is, of course, not in the winding number corresponding to a single trajectory, but rather in the statistics of winding numbers. More concretely, we wish to study the distribution of W , averaged over all paths, with the appropriate Boltzmann weight. The winding number variance for a single polymer with line tension g is

$$\langle W^2 \rangle = \frac{\int \mathcal{D}\mathbf{r}(\tau) \left[\int d\tau [\dot{\mathbf{r}} \cdot \mathbf{A}(\mathbf{r}(\tau))]^2 e^{-\int_0^L \mathcal{L}_0[\mathbf{r}(\tau), \dot{\mathbf{r}}(\tau)] d\tau/T} \right]}{\int \mathcal{D}\mathbf{r}(\tau) e^{-\int_0^L \mathcal{L}_0[\mathbf{r}(\tau), \dot{\mathbf{r}}(\tau)] d\tau/T}}, \quad (3.2)$$

where the free energy density

$$\mathcal{L}_0 = \frac{1}{2}g \left(\frac{d\mathbf{r}}{d\tau} \right)^2 + U(\mathbf{r}) \quad (3.3)$$

plays the role of a Lagrangian in the imaginary time path integral formulation of quantum mechanics. Here, $U(\mathbf{r})$ includes the potential due to the columnar (i.e. τ -independent) disorder and a part representing the excluded volume interaction with the cylinder, as in Eq. (2.15).

Upon defining a new function

$$\mathcal{L}_\nu[\mathbf{r}(\tau), \dot{\mathbf{r}}(\tau)] = \mathcal{L}_0 - iT\nu \frac{d\mathbf{r}}{d\tau} \cdot \mathbf{A}[\mathbf{r}(\tau)], \quad (3.4)$$

we have

$$\langle W^2 \rangle = -\frac{\partial^2}{\partial \nu^2} \ln \mathcal{Z}(\nu)|_{\nu=0}, \quad (3.5)$$

where

$$\mathcal{Z}(\nu) = \int \mathcal{D}\mathbf{r}(\tau) \exp \left[-\frac{1}{T} \int_0^L \mathcal{L}_\nu[\mathbf{r}(\tau), \dot{\mathbf{r}}(\tau)] d\tau \right]. \quad (3.6)$$

It is straightforward using standard path integral manipulations to express $\mathcal{Z}(\nu)$ in terms of $\hat{\mathcal{H}}(\nu)$, the Hamiltonian operator associated with \mathcal{L}_ν ,

$$\hat{\mathcal{H}}(\nu) = \frac{T^2}{2g} \left[\frac{1}{i} \nabla + \nu \mathbf{A}(\mathbf{r}) \right]^2 + U(\mathbf{r}), \quad (3.7)$$

specifically,

$$\mathcal{Z}(\nu) = \text{Tr} \left\{ e^{-\hat{\mathcal{H}}(\nu)L/T} \right\}, \quad (3.8)$$

where the trace means we have now imposed periodic boundary conditions. For a system with cross-sectional area Ω the mean square winding number itself is

$$\langle W^2 \rangle = \frac{L}{\Omega} \frac{\partial}{\partial \nu} \int d\mathbf{r} \langle j_\nu(\mathbf{r}) \rangle \cdot \mathbf{A}(\mathbf{r})|_{\nu=0}, \quad (3.9a)$$

$$\langle W^2 \rangle = \frac{L}{T} \left\langle \frac{\partial^2 \hat{\mathcal{H}}(\nu)}{\partial^2 \nu} \right\rangle_{\nu=0} - \frac{1}{T^2} \int_0^L d\tau \int_0^L d\tau' \left\langle \hat{T} \left[\frac{\partial \hat{\mathcal{H}}}{\partial \nu}(\tau) \frac{\partial \hat{\mathcal{H}}}{\partial \nu}(\tau') \right] \right\rangle_{\nu=0}, \quad (3.9b)$$

where

$$\mathbf{j}_\nu(\mathbf{r}) \equiv -\frac{1}{T} \frac{\partial \hat{\mathcal{H}}}{\partial \mathbf{A}} = \frac{T}{g} \left[\frac{1}{i} \nabla + \nu \mathbf{A}(\mathbf{r}) \right] \quad (3.10)$$

is the current operator, $\langle \hat{O} \rangle \equiv \frac{1}{Z} \text{tr} \{ \hat{O} e^{-\beta \hat{\mathcal{H}}} \}$, \hat{T} is the time ordering operator, and time dependence of operators is defined according to the Heisenberg picture in imaginary time $\hat{O}(\tau) \equiv e^{-\hat{\mathcal{H}}\tau} \hat{O} e^{\hat{\mathcal{H}}\tau}$.

Equations (3.9a,3.9b) are central to our discussion. On the left-hand side they both have the fluctuations in the winding number. On the right-hand side, the first equation has the derivative of the persistent, thermodynamic, current due to a fictitious quantum particle flowing in a multiply connected geometry threaded by an Aharonov-Bohm flux. The derivative is taken with respect to the particle “charge” ν , and the current is weighted by the vector potential. Equation (3.9b) expresses this derivative in terms of one- and two-time particle correlation functions. An analogous equation for *many* directed polymers in terms of boson correlation functions will be given in section IV. Information known from studies of quantum mechanical particles and many particle boson systems regarding these correlation functions will allow us to determine $\langle W^2 \rangle$.

Equations (3.9a,3.9b) are expressions for the variance of the winding number W . We now briefly discuss the probability that the winding number W equals n , denoted by $P_W(n)$. This probability is,

$$P_W(n) = \frac{\mathcal{P}_W(n)}{\sum_n \mathcal{P}_W(n)}, \quad (3.11)$$

where

$$\begin{aligned}
\mathcal{P}_W(n) &= \int D\mathbf{r}(z) \delta \left[\int d\tau \mathbf{A}[\mathbf{r}(z)] \cdot \dot{\mathbf{r}} - n \right] e^{-\int_0^L \mathcal{L}_0[\mathbf{r}(z), \dot{\mathbf{r}}(z)] dz/T} \\
&= \frac{1}{2\pi} \int d\nu \int D\mathbf{r}(\tau) e^{-\frac{1}{T} \int_0^L \mathcal{L}[\mathbf{r}(\tau), \dot{\mathbf{r}}(\tau)] d\tau + i\nu \int_0^L d\tau \mathbf{A}[\mathbf{r}(\tau)] \cdot \dot{\mathbf{r}} - i\nu n} \\
&= \frac{1}{2\pi} \int d\nu \mathcal{Z}(\nu) e^{-i\nu n}
\end{aligned} \tag{3.12}$$

with $\mathcal{Z}(\nu)$ given by (3.6). Equation (3.11) is again a mapping of the statistical property we are interested in onto a quantum mechanical problem, albeit a less transparent one: the probability $P_W(n)$ is proportional to the Fourier transform, with respect to ν , of the quantum mechanical partition function of a particle of charge ν on an Aharonov-Bohm ring threaded by a flux $1/2\pi$. For a related discussion, including an earlier derivation of Eq. (3.12), see Ref. [24].

The normalization of the probability distribution function $\mathcal{P}_W(n)$ is a matter of some subtlety. In the second line of Eq. (3.12) we used the identity,

$$\delta \left[\int d\tau \mathbf{A}[\mathbf{r}(\tau)] \cdot \dot{\mathbf{r}} - n \right] = \frac{1}{2\pi} \int d\nu e^{i\nu \left(\int_0^L d\tau \mathbf{A}[\mathbf{r}(\tau)] \cdot \dot{\mathbf{r}} - n \right)}. \tag{3.13}$$

The limits of the ν integration are determined by the allowed values of the winding number $\int d\tau \mathbf{A}[\mathbf{r}(\tau)] \cdot \dot{\mathbf{r}}$. Since we assume periodic boundary conditions, the allowed trajectories are closed ($\mathbf{r}(0) = \mathbf{r}(L)$), the winding number is an integer, and the integral over ν can be taken between 0 and 2π . However, if the allowed trajectories are not closed, the winding number can be non-integer, and the integral over ν should be taken between $-\infty$ and $+\infty$. For periodic boundary conditions, the integration domain $\nu \in [0, 2\pi]$ leads to $\sum_n \mathcal{P}_W(n) = 1$. Although we have focused on periodic boundary conditions, in the limit $L \rightarrow \infty$ one expects the difference between periodic and open trajectories to vanish.

B. A Single Polymer on a Thin Cylinder

We now specialize to a polymer, whose motion in the $x - y$ plane is confined to a ring of radius a , but is stretched out along the τ axis. The polymer's Lagrangian is given by Eq. (3.3) and we add to $U(\mathbf{r})$ a piece which confines the particle to an *annulus* just outside the

cylindrical barrier of radius a . Our previous discussion maps its random walk around the ring onto the thermodynamics of a quantum charged particle on an Aharonov-Bohm ring. The solenoid's vector potential is then $\mathbf{A} = \frac{\hat{\boldsymbol{\theta}}}{2\pi a} = \text{constant}$, where $\hat{\boldsymbol{\theta}}$ is a unit vector around the ring.

In the absence of disorder, we easily reproduce the expected results. According to Eq. (3.9b) the winding number variance is

$$\langle W^2 \rangle = \frac{LT}{g(2\pi a)^2} [1 - 2L \langle E(\nu = 0) \rangle] \quad (3.14)$$

where $\langle E(\nu = 0) \rangle$ is the average kinetic energy of a chargeless particle on a ring. For a very large L the average energy is, to exponential accuracy, the energy of the ground state, i.e., 0, and $\langle W^2 \rangle = \frac{LT}{(2\pi a)^2 g}$. As expected for a random walk, the variance of the winding number is proportional to the number of steps taken (i.e., proportional to L). The probability distribution $P_W(n)$ is a Gaussian in this limit, as expected [10]. When $L \rightarrow 0$, $\langle E \rangle \rightarrow \frac{1}{2L}$, and $\langle W^2 \rangle \rightarrow 0$.

The presence of a disorder potential $U(\mathbf{r})$ modifies these results in an interesting way. The effect of disorder on

$$\begin{aligned} \langle j_\nu \rangle &= \frac{1}{T} \left\langle \frac{\partial \hat{\mathcal{H}}}{\partial A} \right\rangle \\ &= \frac{-2\pi a}{L} \frac{\partial}{\partial \nu} \ln \mathcal{Z}(\nu), \end{aligned} \quad (3.15)$$

i.e., the persistent current in a mesoscopic ring threaded by an Aharonov-Bohm flux, is well known: the disorder introduces a length scale, ξ , the quantum mechanical localization length of the ground state wave function. As $L \rightarrow \infty$,

$$Z(\nu) \approx \exp[-L\epsilon_0(\nu)/T], \quad (3.16)$$

where $\epsilon_0(\nu)$ is the ground state energy. As a crude, but illuminating model of localization, consider a *single* narrow trap of depth U_0 running up the side of the cylinder. The periodic boundary conditions around the cylinder then lead to a tight-binding model type result for the ground state energy as a function of ν ,

$$\epsilon_0(\nu) = -U_0 - 2t_1 \cos(\nu) - 2t_2 \cos(2\nu) - \dots \quad (3.17)$$

where the couplings t_n represent the matrix elements for tunneling around the cylinder n times, $t_n \sim e^{-2\pi an/\xi}$. For a square well of depth U_0 and size b with $U_0 \gg T^2/2gb^2$ we have (see, e.g. [11]) $\xi \approx T/\sqrt{2gU_0}$ and $t_1 \approx \frac{T^2}{gb^2} e^{-2\pi a/\xi}$. Upon using only the first two terms to evaluate (3.15), we find

$$\langle j(\nu) \rangle = \frac{4\pi at_1}{T} \sin \nu, \quad (3.18)$$

and it follows from Eq. (3.9a) that the mean square winding number behaves as

$$\begin{aligned} \langle W^2 \rangle &= 2t_1 L/T \\ &\sim e^{-2\pi a/\xi} L. \end{aligned} \quad (3.19)$$

Although the variance is still proportional to L , the coefficient $2t_1/T$ which multiplies L vanishes *exponentially* fast as $a \rightarrow \infty$.

C. A Single Polymer on a Thick Cylinder

In the previous section we considered the statistics of winding numbers associated with the motion of a polymer on a thin cylinder or, equivalently, a random walker on a ring. For a more general cylinder of outer radius R , there are two extreme cases, depending on the ratio of the cylinder width $R - a$ and the typical transverse distance the polymer crosses in “time” L , namely $\sqrt{LT/g}$. In the previous section this ratio was zero. Suppose now that this ratio to be small, but nonzero, i.e. $0 < \frac{g(R-a)^2}{TL} \ll 1$. When using eigenfunctions of $\hat{\mathcal{H}}$ to evaluate winding numbers, this condition implies that the partition function has significant contributions only from one radial mode, the one contributing the lowest energy. In this limit, the density profile in the radial direction can be approximated by a constant, and an analysis similar to that following Eq. (3.14) leads, for a disorder-free sample in the limit $L \rightarrow \infty$, to

$$\langle W^2 \rangle = \frac{LT}{g\pi(R^2 - a^2)} \log \frac{R}{a}. \quad (3.20)$$

The opposite limit, in which the cylinder width is essentially infinite, was considered, also in the absence of disorder, in Refs. [4] and [10]. Here, we confine ourselves to a simplified discussion of $\langle W^2 \rangle$ using the quantum formalism. According to Eq. (3.2), the variance $\langle W^2 \rangle$ can be written,

$$\langle W^2 \rangle = \int_0^L d\tau \int_0^L d\tau' \left\langle \frac{dr_i(\tau)}{d\tau} \frac{dr_j(\tau')}{d\tau'} A_i[\mathbf{r}(\tau)] A_j[\mathbf{r}(\tau')] \right\rangle. \quad (3.21)$$

Upon approximating the average in the integrand,

$$\begin{aligned} \left\langle \frac{dr_i(\tau)}{d\tau} \frac{dr_j(\tau')}{d\tau'} A_i[\mathbf{r}(\tau)] A_j[\mathbf{r}(\tau')] \right\rangle &\approx \left\langle \frac{dr_i(\tau)}{d\tau} \frac{dr_j(\tau')}{d\tau'} \right\rangle \langle A_i[\mathbf{r}(\tau)] A_j[\mathbf{r}(\tau')] \rangle \\ &\approx \frac{2T}{g} \delta(\tau - \tau') \langle A^2[\mathbf{r}(\tau)] \rangle, \end{aligned} \quad (3.22)$$

we have

$$\langle W^2 \rangle = \frac{2T}{g} \int_0^L d\tau \int d^2r \mathcal{P}(\mathbf{r}, \tau) A^2(\mathbf{r}), \quad (3.23)$$

where $\mathcal{P}(\mathbf{r}, \tau)$ is the probability of finding the random walker at position \mathbf{r} at height τ . For an infinitely thick cylinder, we have $P(\mathbf{r}, \tau) = \frac{g}{2\pi T\tau} e^{-gr^2/2T\tau}$ and $\langle W^2 \rangle \propto (\log L)^2$. The thermal averages in Eq. (3.9a,3.9b) now include many eigenstates.

The effect of disorder can also be understood by a similar analysis. Again, disorder introduces a localization length ξ , characterizing the eigenstates of the Hamiltonian $H(\nu)$. As long as ξ is larger than the cylinder's size, the effect of the disorder is weak. When ξ is smaller than the cylinder's outer radius, but larger than $2\pi a$, its inner circumference, the effective outer radius of the cylinder becomes ξ . Points on the plane whose distance from the obstacle is larger than ξ support mostly eigenstates that are insensitive to ν . Thus, they do not contribute to the winding number. Particles that start their way at such points never make it to the hole. Therefore, the winding number for such a system becomes,

$$\langle W^2 \rangle \propto \begin{cases} (\log L)^2 & \text{for } \frac{TL}{g} < \xi^2, \quad \xi > 2\pi a, \\ \frac{L}{\xi^2} \log\left(\frac{\xi}{a}\right) & \text{for } \frac{TL}{g} > \xi^2, \quad \xi > 2\pi a \end{cases}. \quad (3.24)$$

Finally, when $\xi < 2\pi a$ the contribution to the winding number comes from a 1-D strip around the hole, and the 1-D result applies, namely $\langle W^2 \rangle \propto e^{-2\pi a/\xi} L$. To summarize,

for an infinitely wide cylinder in the long-time limit disorder makes the winding number increase, for particles that start their random walk close enough to the hole. In the absence of disorder the particles diffuse away from the hole, and thus end up with a small rate of winding. Disorder prevents them from diffusing away from the hole, and increases the winding number.

IV. WINDING STATISTICS OF MANY POLYMERS

We now turn to discuss a system with many polymers (or flux lines). As discussed in section 2, the two-dimensional Hamiltonian which describes the physics is that of interacting bosons, interacting both mutually and with randomly placed pinning centers. The pinning centers we discuss here are assumed to result from columnar defects, and thus create a τ -independent potential.

The Hamiltonian is a generalization of Eq. (2.13), namely,

$$\hat{\mathcal{H}} = \frac{T^2}{2g} \sum_{j=1}^N \left[\frac{1}{i} \nabla_j + \nu \mathbf{A}(\mathbf{r}_j) \right]^2 + \sum_{j=1}^N U(\mathbf{r}_j) + \sum_{i>j} V(|\mathbf{r}_i - \mathbf{r}_j|) \quad (4.1)$$

where V is the interaction potential and U includes both disorder and the interaction with a repulsive cylinder centered on the origin. Note that neither V nor U depend on ν , which determines only the coupling of the bosons to the Aharonov-Bohm flux. The phase diagram of the Hamiltonian (4.1) includes several phases, most notably a superfluid phase and an insulating bose glass phase in the limit $L \rightarrow \infty$. The properties of these phases are reflected in the winding number distributions. The winding number for many directed lines is given by Eq. (2.17), and the many particle generalization of Eq. (3.9b) is

$$\begin{aligned} \langle W^2 \rangle = \frac{TL}{g} \int d^2r \langle n(\mathbf{r}) \rangle A^2(r) - \int_0^L d\tau \int_0^L d\tau' \int d^2r \int d^2r' \langle \hat{T}[j_\alpha(\mathbf{r}, \tau) j_\beta(\mathbf{r}', \tau')] \rangle_{\nu=0} \\ \times A_\alpha(\mathbf{r}) A_\beta(\mathbf{r}'). \end{aligned} \quad (4.2)$$

Several comments are in place regarding Eq. (4.2). First, the density operator $n(\mathbf{r}) = \sum_i \delta(\mathbf{r} - \mathbf{r}_i)$ describes the *total* density of particles (rather than, e.g., the superfluid density).

Second, the current-current correlation function should be calculated for $\nu = 0$, i.e., the current operator is $j_\alpha(\mathbf{r}) = (1/2g) \sum_i [\delta(\mathbf{r} - \mathbf{r}_i) p_\alpha + p_\alpha \delta(\mathbf{r} - \mathbf{r}_j)]$. Finally, the interpretation of the second term becomes clearer upon Fourier transformation. After Fourier analysis, the imaginary-time current-current correlation function appearing on the right-hand side of Eq. (4.2) becomes the linear response function $\chi_{\alpha\beta}(\mathbf{q}, \omega = 0)$ defined by $j_\alpha(\mathbf{q}, \omega = 0) = \sum_\beta \chi_{\alpha\beta}(\mathbf{q}, \omega = 0) A_\beta(\mathbf{q}, \omega = 0)$, i.e., the function describing the current response to a weak, time-independent vector potential [25].

The current-current correlation function $\chi_{\alpha\beta}(\mathbf{r}, \tau) = \langle \hat{T}[j_\alpha(\mathbf{r}, \tau) j_\beta(\mathbf{0}, 0)] \rangle$ in Eq. (4.2) may be decomposed in longitudinal and transverse parts. The corresponding Fourier decomposition reads

$$\chi_{\alpha\beta}(\mathbf{r}, \tau) = \frac{1}{\Omega L} \sum_{\mathbf{q}, \omega} e^{i\mathbf{q}\cdot\mathbf{r} - i\omega\tau} \left[\chi_{\parallel}(\mathbf{q}, \omega) \frac{q_\alpha q_\beta}{q^2} + \chi_{\perp}(\mathbf{q}, \omega) \left(\delta_{\alpha\beta} - \frac{q_\alpha q_\beta}{q^2} \right) \right]. \quad (4.3)$$

However, the vector potential $\mathbf{A}(\mathbf{r}) = \frac{\hat{\tau} \times \mathbf{r}}{2\pi r^2}$ for winding around an obstacle is purely transverse, so only $\chi_{\perp}(\mathbf{q}, \omega)$ contributes to the winding number. Upon passing to the limit of large system dimensions in the xy -plane, and rewriting the second term of (4.2) in Fourier space, we have

$$\langle W^2 \rangle = \frac{TL}{g} \int d^2r \langle n(\mathbf{r}) \rangle A^2(\mathbf{r}) - L \int \frac{d^2q}{(2\pi)^2} \chi_{\perp}(\mathbf{q}, \omega = 0) |\hat{\mathbf{A}}(\mathbf{q})|^2 \quad (4.4)$$

where $\hat{\mathbf{A}}(\mathbf{q})$ is the Fourier transform of $\mathbf{A}(\mathbf{r})$.

$$\hat{\mathbf{A}}(\mathbf{q}) = \frac{-i\hat{\tau} \times \mathbf{q}}{|\mathbf{q}|^2}. \quad (4.5)$$

Suppose the directed polymers are confined in an annulus of outer radius $R \gg a$, where a is the radius of the cylindrical obstacle. As $R \rightarrow \infty$, we can neglect any distortion of the line density due to the obstacle and approximate $\langle n(r) \rangle$ by its average value, n , far from the inner boundary. The first term of Eq. (4.4) then behaves like $\frac{TL}{2\pi g} n \ln(R/a)$, i.e., it diverges logarithmically with coefficient proportional to the average density of lines. Because $|\hat{\mathbf{A}}(\mathbf{q})|^2 = 1/q^2$, the integral in the second term is dominated by the behavior of $\chi_{\perp}(q, \omega = 0)$ in the limit $q \rightarrow 0$. Upon imposing upper and lower Fourier cutoffs of a^{-1} and R^{-1} , we *again*

find a logarithmically diverging contribution to the winding number, and the mean square winding number in the large R limit is

$$\langle W^2 \rangle = \frac{TL}{2\pi g} n \ln(R/a) - \frac{L}{2\pi} \left[\lim_{q \rightarrow 0} \chi_{\perp}(q, \omega = 0) \right] \ln(R/a). \quad (4.6)$$

However, the transverse response function $\chi_{\perp}(q, \omega)$ is well known to be related to the *normal* density n_n of the equivalent system of interacting bosons [16,23]

$$\lim_{\mathbf{q} \rightarrow 0} \chi_{\perp}(\mathbf{q}, \omega = 0) = \frac{T}{g} n_n. \quad (4.7)$$

Upon defining the superfluid number density $n_s = n - n_n$, we are led to our final result, namely

$$\langle W^2 \rangle = \frac{TL}{2\pi g} n_s \ln(R/a). \quad (4.8)$$

Equation (4.8) is an exact relation, valid in the limit $R \gg a$, between winding number fluctuations and the superfluid density of the equivalent boson system. When reexpressed in terms of the boson parameters of section 2 it reads

$$\langle W^2 \rangle = \frac{n_s \hbar^2}{2\pi m k_B T} \ln(R/a), \quad (4.9)$$

which is similar in some respects to the Pollock-Ceperley result (2.9) for boson world lines winding around a torus [26]. Unlike the Pollock-Ceperley formula, however, Eq. (4.8) applies directly to a real physical system, namely “directed polymer melts” composed of vortex lines in Type II superconductors with columnar defects. As discussed in section 2, $\langle W^2 \rangle$ determines the linear response of the net winding number to a current through the obstacle.

According to Eq. (4.8) the winding number fluctuation around an obstacle for many interacting directed polymers is predicted to diverge linearly with the length of the obstacle and logarithmically with the cross-sectional area, as one might guess by multiplying the result (3.20) for a single polymer in a moderately thick cylinder by N . The meaning of the coefficient becomes clearer if we first define a “thermal deBroglie wavelength“ Λ_T for the polymers by

$$\Lambda_T^2 = \frac{2\pi TL}{g}, \quad (4.10)$$

i.e., the directed polymer analogue of Eq. (2.7) with the usual identifications $\hbar \rightarrow T$, $\hbar/T \rightarrow L$ and $m \rightarrow g$. This length is a measure of the transverse wandering distance of the polymers as they traverse the sample. Equation (4.8) then becomes

$$\langle W^2 \rangle = \left(\frac{\Lambda_T}{2\pi} \right)^2 n_s \ln(R/a), \quad (4.11)$$

showing that only a part of the “superfluid fraction” n_s of lines, i.e., those within a transverse wandering distance of the obstacle, contribute to the winding number fluctuations. Correlated disorder along the $\hat{\tau}$ axis should decrease the winding number fluctuations. Equation (4.11) shows that this reduction is given entirely by the corresponding reduction in the superfluid density. The reduction in n_s for directed lines subjected to various kinds of correlated disorder is calculated explicitly in Ref. [23].

ACKNOWLEDGMENTS

It is a pleasure to acknowledge helpful conversations with D. Bishop and D. Ceperley. Work by DRN was supported by the National Science Foundation, primarily by the MRSEC program through Grant DMR-9400396 and in part through Grant DMR-9417047.

*To appear in Proceedings of the XIV Sitges Conference, “Complex Behavior of Glassy Systems,” June 10-14, 1996, edited by M. Rubi.

REFERENCES

- [1] S.F. Edwards, Proc. Phys. Soc. **91**, 513 (1967) J. Phys. **A1**, 15 (1968).
- [2] S. Prager and H.L. Frisch, J. Chem. Phys. **46**, 1475 (1967).
- [3] For a review, see A. Grossberg and A. Khoklov, in Advances in Polymer Science **106**, 1 (1993).
- [4] J. Rudnick and Y. Hu, J. Phys. A. Math. Gen. **20**, 4421 (1987).
- [5] Y. Aharonov and D. Bohm, Phys. Rev. **115**, 485 (1959).
- [6] E.L. Pollack and D.M. Ceperley, Phys. Rev. **B36**, 8843 (1987).
- [7] For a review, see D.M. Ceperley, Rev. Mod. Phys. **67**, 279 (1995).
- [8] G. Blatter, M.V. Feigel'man, V.B. Geshkenbein, A.I. Larkin, and V. Vinokur, Reviews of Modern Physics **66**, 1125 (1994).
- [9] D.R. Nelson and S. Seung, Phys. Rev. **B39**, 9153 (1989), D.R. Nelson and P. Le Doussal, Phys. Rev. **B42**, 10113 (1990).
- [10] B. Drossel and M. Kardar, Phys. Rev. **E53**, 5861 (1996); and cond-mat/96100119.
- [11] D.R. Nelson and V. Vinokur, Phys. Rev. **B48**, 13060 (1993).
- [12] Z. Yao, S. Yoon, H. Dai, S. Fan and C.M. Lieber, Nature **371**, 777 (1995).
- [13] We assume currents so small that the structure of the Bose glass state inside the tube is unaffected, due to the transverse Meissner effect [11]. For strong enough currents, the Bose glass in the tube may deform slightly, thus forming a repulsive *chiral* defect, similar to that discussed by Drossel and Kardar [10].
- [14] R.P. Feynman, *Statistical Mechanics* (Benjamin, Reading, MA, 1972).
- [15] R.P. Feynman, Phys. Rev. **91**, 1291 (1953).

- [16] P. Nozieres and D. Pines, *The Theory of Quantum Liquids*, vol. 2 (Addison-Wesley, Reading 1990).
- [17] D.R. Nelson and J.M. Kosterlitz, Phys. Rev. Lett. **39**, 1201 (1977).
- [18] See, e.g., R. Bellissent, L. Descotes and P. Pfeuty, Journal of Physics C**6**, Suppl. A211 (1994).
- [19] For reviews, see D.R. Nelson, Physica A**177**, 220 (1991); and D.R. Nelson in *Observation, Prediction and Simulation of Phase Transition in Complex Fluids*, edited by Ml. Bans et al. (Kluwer, The Netherlands, 1995).
- [20] See, e.g., M.P.A. Fisher and D.H. Lee, Phys. Rev. B**39**, 2756 (1989).
- [21] P.G.. deGennes, *Superconductivity of Metals and Alloys* (Addison-Wesley, Reading, MA 1989), chapter 2.
- [22] See., e.g., V.G. Kogan, Phys. Rev. B**24**, 1572 (1981).
- [23] U. Tauber and D.R. Nelson, submitted to Physics Reports.
- [24] A. Comtet, J. Desbois and S. Ouvry J. Phys. Math Gen. **23**, 3563 (1990); A. Comtet, J. Desbois and C. Monthus J. Stat. Phys. **73**, 433 (1993); B. Houchmandzadeh, J. Lajzerowicz and M. Vallade J. de Physique 1 **2**, 1881 (1992).
- [25] G.D. Mahan, *Many-Particle Physics* (Plenum Press, New York 1981), sections (3.3) and (3.7).
- [26] By taking $\mathbf{A}(\mathbf{r}) = \text{const.}$ in Eq. (4.2), one easily derives the Pollock-Ceperley formula (2.9) for bosons on a torus.

FIGURES

FIG. 1. Slab of Type II superconductor with a dense array of columnar pins confined to a cylinder with a dilute concentration of columnar defects outside. Vortices inside the cylinder are in the Bose glass phase, while those outside are free to move and entangle in a flux liquid.

FIG. 2. Effect of a current through a cylindrical obstacle on a flux liquid. The lines wind around the obstacle with a preferred chirality when the current is on.

FIG. 3. Boson trajectories in $2 + 1$ dimensions projected onto the xy -plane. Three trajectories with characteristic interparticle distance a and four images of the periodic box of size D are shown. The periodic boundary conditions in the time-like direction mean that only small ring trajectories appear in the high temperature image at left. Trajectories which cross between the periodic cells and lead to nonzero winding numbers are shown in the low-temperature image on the right.

FIG. 4. Mean square winding number $\langle \mathbf{W}^2 \rangle$ for bosons in $2 + 1$ dimensions a function of $\beta = 1/k_B T$. A Kosterlitz-Thouless transition occurs for $\beta = \beta_c$. Dashed line is the corresponding quantity for directed polymer melts.

FIG. 5. Trajectories for directed polymer melts with “open” boundary conditions at the top and bottom of a slab of thickness L .

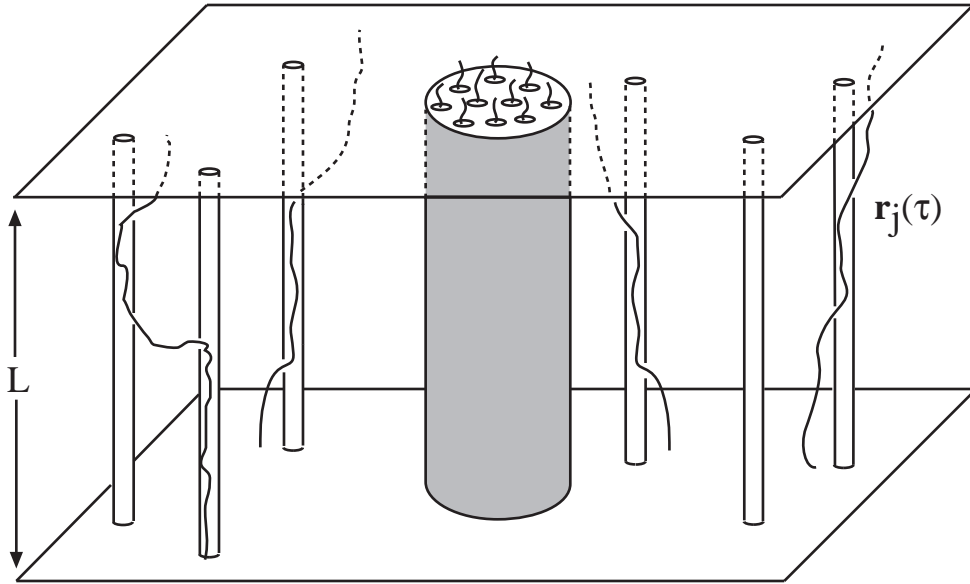


FIG. 1

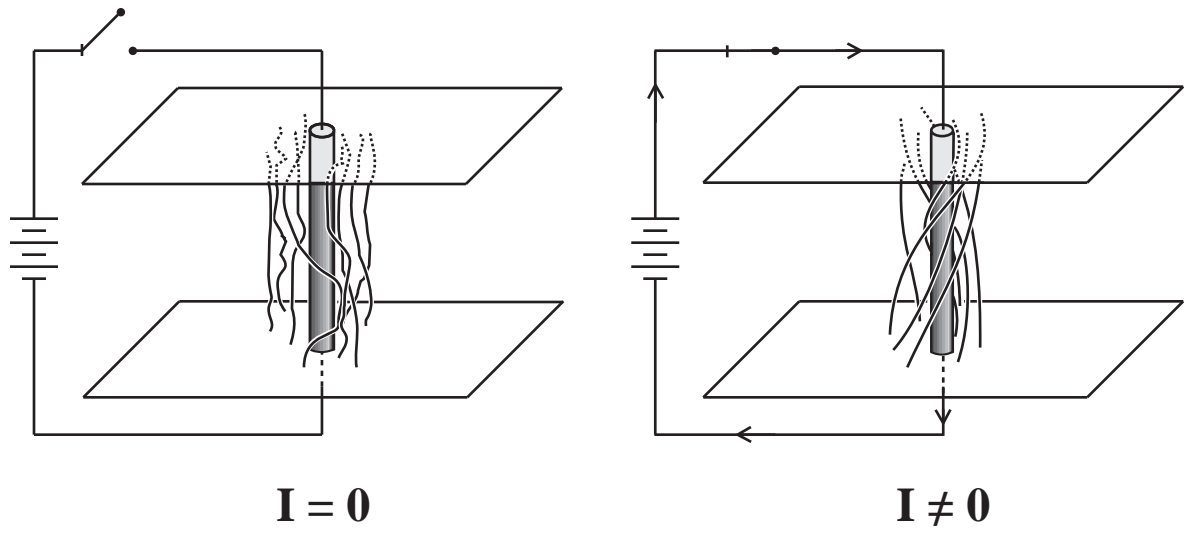
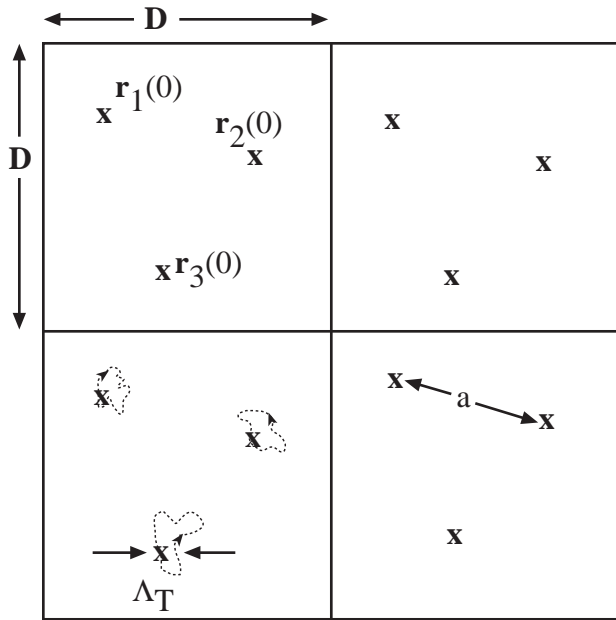
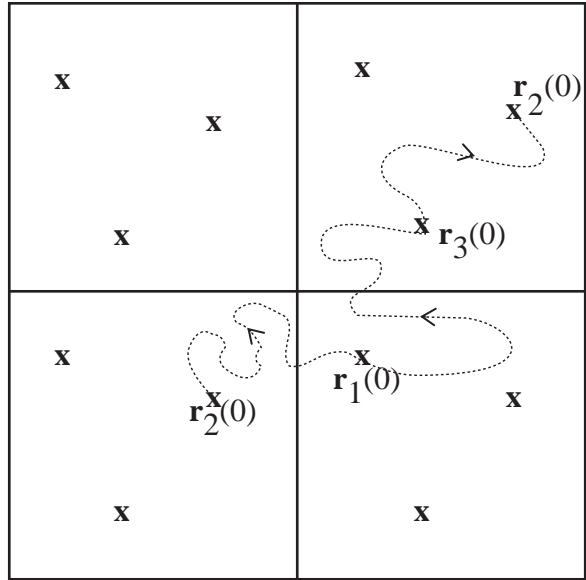


FIG. 2



high T ($\Lambda_T \ll a \ll D$)

$$\mathbf{W} = (0,0)$$



low T ($a \ll \Lambda_T \ll D$)

$$\mathbf{W} = (1,1)$$

FIG. 3

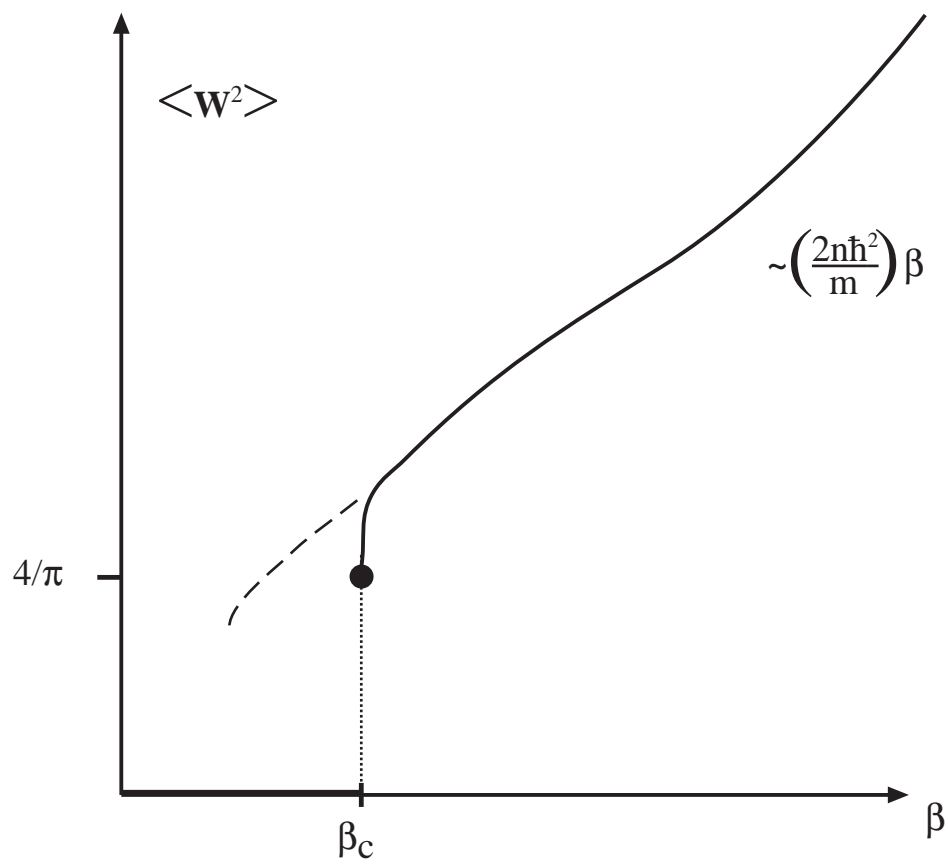


FIG. 4

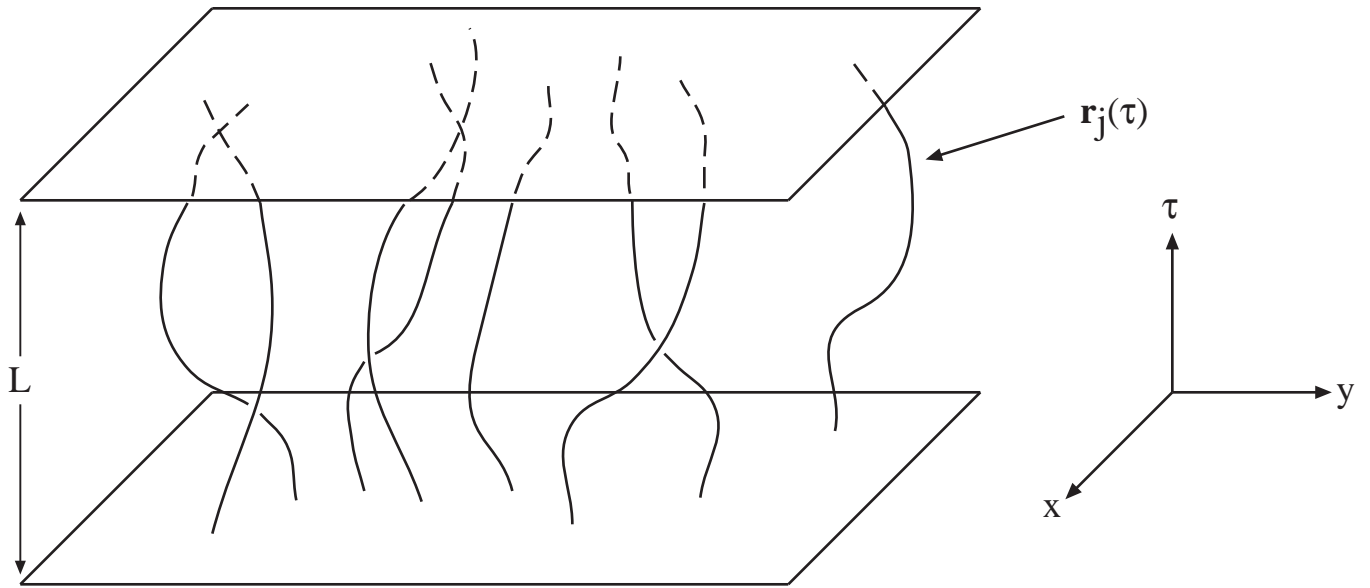


FIG. 5